



Timing and Structure of the 4.2 ka BP Event in the Indian Summer Monsoon Domain from an Annually-Resolved Speleothem Record from Northeast India

5 Gayatri Kathayat^{1*}, Hai Cheng^{1, 2*}, Ashish Sinha³, Max Berkelhammer⁴, Haiwei Zhang¹, Pengzhen Duan¹, Hanying Li¹, Xiangley Li¹, Youfeng Ning¹, Richard Lawrence Edwards²

¹ Institute of Global Environmental Change, Xi'an Jiaotong University, China

² Department of Earth Sciences, University of Minnesota, Minneapolis, USA

³ Department of Earth Science, California State University Dominguez Hills, Carson, USA

10 ⁴ Department of Earth and Environmental Sciences, University of Illinois, Chicago, USA

Correspondence to: Gayatri Kathayat (kathayat@xjtu.edu.cn) & Hai Cheng (cheng021@xjtu.edu.cn).

Abstract

15 A large array of proxy records suggests that the '4.2 ka event' marks an ~300-year period of major global climate anomaly. However, the climatic manifestation of this event, including its onset, duration, and termination, remain less clear in the Indian summer monsoon (ISM) domain. Here, we present a new speleothem oxygen isotope ($\delta^{18}\text{O}$) record from Mawmluh Cave, Northeast India, which provides an annually-resolved record of
20 changes in ISM strength between ~4.440 and 3.780 ka BP. Our $\delta^{18}\text{O}$ record is constrained by 18 ^{230}Th dates with an average age uncertainty of ± 13 years and a dating resolution of ~40 years, which allow us to characterize the timing and structure of the '4.2 ka event' with an unprecedented detail. The overall expression of the 4.2 ka event in our record shares broad similarities with a previous $\delta^{18}\text{O}$ record from the Mawmluh Cave as well as
25 with other previous lower-resolution proxy reconstructions of the ISM. However, unlike some previous ISM records, where the '4.2 ka event' has been described as a singular multi-centennial period of anomalously weak ISM, our data suggest a more variable nature of ISM during this period. The '4.2 ka event' in our record exhibits a three-stage structure, characterized by highly variable ISM between ~4.255 and 4.070 ka BP and a
30 distinct pluvial phase from ~4.070-4.010 ka BP. The latter abruptly (<10 years) culminated into a relatively weaker phase of ISM, which was punctuated by a number of multidecadal periods of anomalously drier condition. While our record shows evidence of a discernible beginning of the 4.2 ka event, there is no clear evidence of its 'end' thus, suggesting that the ISM experienced a major regime-shift or transition at ~4.0 ka BP.

35



1. Introduction

The interval between 4.2 and 3.9 ka BP (thousand years before present, where present =1950 AD) constitutes an important period of time from both climatological and archeological perspectives (e.g., Weiss et al.,1993; Cullen et al., 2000; Staubwasser et al., 2003; Berkelhammer et al., 2012). A global suite of proxy records shows widespread climate anomalies during this time (commonly referred as the ‘4.2 ka event’) (e.g., Cullen et al., 2000; Staubwasser et al., 2003; Arz et al., 2006; Drysdale et al., 2006; Menounos et al., 2008; Liu and Feng, 2012; Berkelhammer et al., 2012; Dixit et al., 2014; Cheng et al. 2015; Nakamura et al., 2016; Dixit et al., 2018; Railsback et al., 2018). Additionally, a number of archeological studies also suggest that the ‘4.2 ka event’ may have been associated with a series of cultural and societal changes in the Mediterranean, Middle East, Africa, South and East Asia (e.g., Weiss et al.,1993; Enzel et al., 1999; Cullen et al., 2000; Staubwasser et al., 2003; Marshall et al., 2011; Liu and Feng, 2012; Dixit et al., 2014; Weiss, 2016). For example, the ‘4.2 ka event’ has been proposed to have contributed to collapses of the early Bronze age civilizations, including the Longshan Culture in China (Change, 1999; Liu and Feng, 2012), Egyptian Old Kingdom by the Nile River (Stanley et al., 2003), and the Akkadian Empire in Mesopotamia (Weiss et al.,1993; Cullen et al., 2000). In South Asia, the 4.2 ka event has been linked to a weakening of the Indian summer monsoon (ISM) and the ensuing deurbanization of the Indus Valley Civilization (Staubwasser et al., 2003; Madella and Fuller, 2006; Dixit et al., 2014; Giosan et al., 2012; Berkelhammer et al., 2012; Kathayat et al., 2017; Dixit et al., 2018).

A number of proxy records from the Indian subcontinent suggest that a major weakening of ISM occurred during the ‘4.2 ka event’ (Staubwasser et al., 2003; Berkelhammer et al., 2012; Ponton et al., 2012., Dixit et al., 2014; Nakamura et al., 2016; Hong et al 2014; Hong et al., 2016; Shukla et al., 2018) (Fig. 1).

This event has been generally described as an approximately a two centuries-long interval of aridity, which was superimposed on a long-term gradually declining trend in ISM in response to decreasing northern hemisphere summer insolation (e.g., Kathayat et al., 2017). However, the timing, structure and magnitude of the 4.2 ka event in the ISM regime remain unclear. For example, while a speleothem record from Mawmluh Cave in Northeast India shows an abrupt onset of the event at ~4.1 ka BP (Berkelhammer et al., 2012), the onset/duration timings of the 4.2 ka event in other records differ considerably (e.g., Staubwasser and Weiss, 2006; Prasad and Enzel, 2006; Nakamura et al., 2016; Dixit et al., 2018). Furthermore, a speleothem oxygen isotope ($\delta^{18}\text{O}$) record from Sahiya Cave, North India



70 (Kathayat et al., 2017) indicates a long-term drying trend in ISM from ~4200 to 3500 years but does not contain a clear expression of the event.

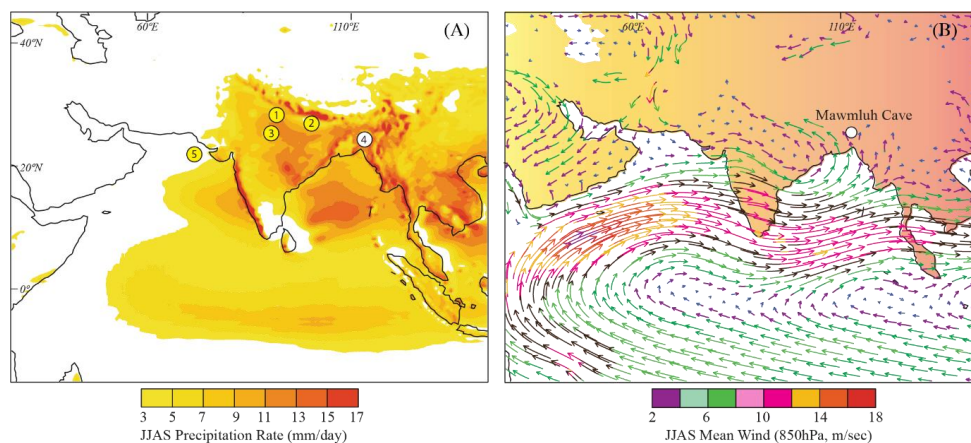


Figure 1. Location map and spatial structure of mean JJAS precipitation and low-level winds. (A) JJAS precipitation from the Tropical Rainfall Measuring Mission (TRMM). The locations of Mawmluh Cave (white circle) and other proxy records mentioned in the text (yellow circles and numbers). The numbering scheme is as follows: 1, Sahiya cave (Kathayat et al., 2017); 2, Lake Rara (Nakamura et al., 2016); 3, Kotla Dhar (Dixit et al., 2014); 4, Mawmluh Cave (Berkelhammer et al., 2012); and 5, Indus Delta (Staubwasser et al., 2003). (B) 850 hPa-level monsoon vector from zoomed Laboratoire de Meteorologie Dynamique (LMDZ) general circulation model with telescoping zooming (figure adapted and modified from Sabin et al., 2013). The zoom version shows a well-defined cyclonic circulation with westerlies on the southern flanks and easterly winds on the northern flanks of the Monsoon Trough. The Mawmluh Cave is ideally located to record upstream variations in the overall strength of the ISM (see text).

85

However, the latter may also stem from relatively large age uncertainties and low temporal resolution of the Sahiya Cave record around this time interval, which preclude a definitive assessment of the ‘4.2 ka event’ (Kathayat et al., 2017).

A high resolution (~6 years) $\delta^{18}\text{O}$ record from Mawmluh Cave (KM-A), Northeast India has previously provided a clear evidence of the ‘4.2 ka event’ from the ISM domain (Berkelhammer et al. 2012). The 4.2 ka event in the KM-A record event can be described as a ‘pulse-like’ change in the ISM, characterized by a sharp increase in the speleothem $\delta^{18}\text{O}$ values (implying weaker ISM) at ~4.07 ka, which was followed by a large and abrupt decrease in the $\delta^{18}\text{O}$ values at 3.88 ka BP. However, the exact timing and structure of the 4.2 ka event from the KM-A sample has some uncertainty associated with the fact that it is only constrained by only two ^{230}Th dates. Furthermore, the termination of the event occurs near the top ~2 mm

95



portion of KM-A, where the $\delta^{18}\text{O}$ values may have been potentially influenced by recent morphological changes in the shape of KM-A stalagmite. Here, we provide two new replicated speleothem $\delta^{18}\text{O}$ records from Mawmluh Cave (ML.1 and ML.2) (Fig. 2) with an average $\delta^{18}\text{O}$ resolutions of ~ 1 and ~ 5 -year, respectively.

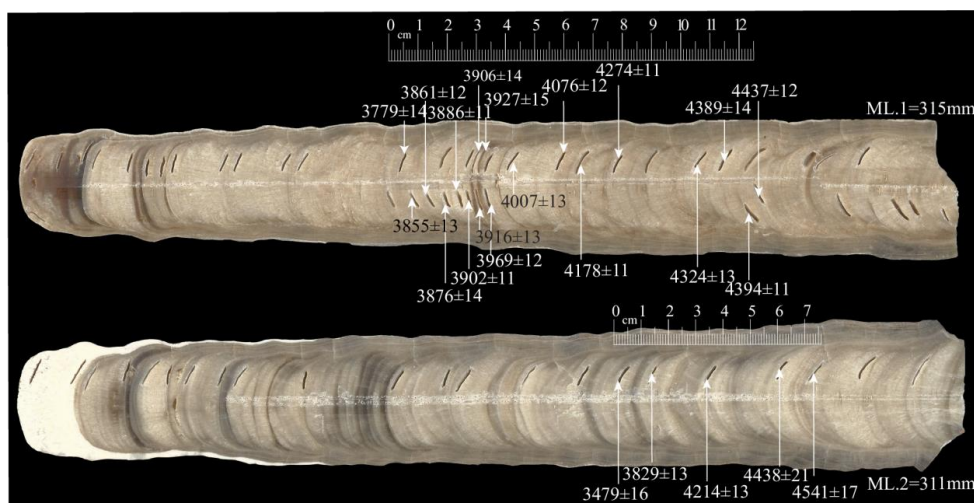


Figure 2. Samples photograph: The total length of ML.1 and ML.2 samples is 315 & 311mm respectively. The arrows indicate the dating sub-sampling location and the ^{230}Th dates with the 2σ analytical error (also see Supplementary Table 1). The cm scale indicates the location of isotopic measurements, enclosing the interval of interest within both the samples.

The ML.1 and ML.2 $\delta^{18}\text{O}$ records span from 4.440 to 3.780 ka BP and 4.530 to 3.370 ka BP, respectively. Our new record is sub-annually to annually resolved, has precise chronologic constraints. The ML.1 and ML.2 chronologies are established by 18 ^{230}Th dates with age uncertainty of $\sim \pm 13$ years (average dating resolution of ~ 40 years) and 5 ^{230}Th dates with age uncertainty of $\sim \pm 16$ years, respectively (Fig. 3) (also see Supplementary Table 1), which allow us to precisely characterize the timing, structure, and manifestation of the 4.2 ka event in the ISM regime. Particularly, we aim to provide better constraints on the timing of the onset of the event and refine the nature of the event's termination.

115

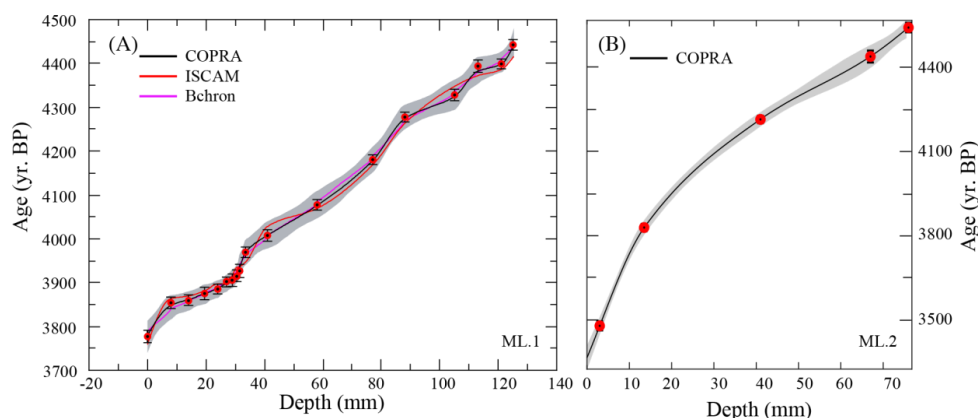


Figure 3. Age Models of ML.1 and ML.2 records. We adopted COPRA and generated 2000 realizations of age models to account for the dating uncertainties (2.5 and 97.5% quantile) confidence limits. (A) ML-1 age models and modeled age uncertainties using 3 different age-modeling algorithms, COPRA (black), Bchron (purple) and ISCAM (red). The gray band depicts the 95% confidence interval using COPRA. Error bars on ^{230}Th dates represent a 2σ analytical error. (B) ML-2 age model and modeled age uncertainties using COPRA.

125 2 Samples and Methods

2.1 Cave location, climatology & characteristics

Mawmluh Cave ($25^{\circ}15'32''\text{N}$, $91^{\circ}42'45''\text{E}$, 1290 m asl) is located near the town of Sohra (Cherrapunji) at the southern fringe of the Meghalaya Plateau, Northeast India (Fig. 1). The mean annual rainfall is $\sim 11,000$ mm in the region, 70% of precipitation falls during the peak ISM months (June–September) (Murata et al., 2007). The rainfall at the cave site during the ISM period is mainly produced by convective systems and the low-level air parcels originated from the Bay of Bengal, which propagates further northward and penetrate deep into the Tibetan Plateau (Breitenbach et al., 2010; Sengupta and Sarkar, 2006). The non–monsoonal component of the rainfall is trivial and consists of the westerly related moisture as well as recycled local moisture (Breitenbach et al., 2010 and 2015; Berkelhammer et al., 2012). The cave is overlain by ~ 30 – 100 m thick and heavily karstified host rock (limestone, sandstone, and a ~ 40 – 100 cm thick coal layer) (Breitenbach et al., 2010). The soil layer above the cave is rather thin (5–15 cm) and covered mainly by grasses and bushes. The cave monitoring data (Breitenbach et al., 2010) indicate that the relative humidity inside the cave is more than 95% even during the dry season (November to April). The temperature variations in the cave are small (18.0 – 18.5°C) and close to the mean annual temperature of the area (Breitenbach et al., 2010 and 2015). A 3-year monitoring study in Mawmluh Cave (Breitenbach et al., 2010)



suggests that drip-water $\delta^{18}\text{O}$ signals in the cave lag the local rainfall by less than 1 month, and thus preserves the seasonal signal of ISM rainfall. Previous studies have indicated that variations in the $\delta^{18}\text{O}$ of speleothem calcite from Mawmluh Cave reflect changes in the amount-weighted $\delta^{18}\text{O}$ of precipitation ($\delta^{18}\text{O}_p$) values (Breitenbach et al., 2010 and 2015; Berkelhammer et al., 2012; Myers et al., 2015; Dutt et al., 2015).

2.2 Proxy Interpretation

The temporal $\delta^{18}\text{O}$ variations in monsoonal rainfall and consequently in speleothem in the study area have been previously interpreted to dominantly reflect spatially-integrated upstream changes in the ISM strength (Sinha et al., 2011; Berkelhammer et al., 2012). A number of studies with isotope-enabled general circulation models (GCMs) also suggest a significant inverse relationship between ISM upstream summer (June to September) rainfall amount and $\delta^{18}\text{O}_p$ variations over the Indian Subcontinent (e.g., Vuille et al., 2005; Pausata et al., 2011; Berkelhammer et al., 2012; Sinha et al., 2015; Midhun and Ramesh, 2016). As such, the low and high $\delta^{18}\text{O}$ values of our records are used to refer to strong and weak monsoons, respectively, consistent with a number of previous studies (e.g., Dayem et al., 2010; Breitenbach et al., 2010; Sinha et al., 2011; Cheng et al., 2012; Sinha et al., 2011; Berkelhammer et al., 2012; Breitenbach et al., 2015; Myers et al., 2015, Dutt et al., 2015; Cheng et al., 2012; Kathayat et al., 2016; Kathayat et al., 2017).

2.3 Samples preparation

The ML.1 and ML.2 samples from Mawmluh Cave were collected ~4–5 m above the cave floor in November 2015 ~700 meters from the cave entrance. The diameters of ML.1 and ML.2 are ~170 and 165 mm, and the length ~315 and ~311 mm, respectively. Both stalagmite samples were cut along their growth axes, using a thin diamond blade. The sub-samples for isotopic measurements for the ML.1 and ML.2 samples were obtained from depths between ~125–250 mm and ~182–255 mm (with respect to the top), respectively. Accordingly, we report our data with depths of zero set at 125 mm and 182 mm from the top for samples ML.1 and ML.2, respectively. Both samples do not have any visible changes in the texture or hiatuses in the above intervals for this study (Fig. 2).



2.4 ^{230}Th dating

175 Subsamples from ML.1 and ML.2 for ^{230}Th dating (~30 mg) were drilled using a 0.5 mm
carbide dental drill. The ^{230}Th dating was performed at the Xi'an Jiaotong University, China
using Thermo-Finnigan Neptune-*plus* multi-collector inductively coupled plasma mass
spectrometers (MC-ICP-MS). The methods were described in Cheng et al., 2000 and 2013).
We used standard chemistry procedures (Edwards et al., 1987) to separate uranium and thorium.
180 A triple-spike (^{229}Th - ^{233}U - ^{236}U) isotope dilution method was used to correct instrumental
fractionation and to determine U/Th isotopic ratios and concentrations (Cheng et al., 2000;
Cheng et al., 2013). U and Th isotopes were measured on a MasCom multiplier behind the
retarding potential quadrupole in the peak-jumping mode using the standard procedures (Cheng
et al., 2000). Uncertainties in U/Th isotopic measurements were calculated offline at 2σ level,
185 including corrections for blanks, multiplier dark noise, abundance sensitivity, and contents of
the same nuclides in spike solution. The U decay constants are reported in Cheng et al. (2013).
Corrected ^{230}Th ages assume the initial $^{230}\text{Th}/^{232}\text{Th}$ atomic ratio of $4.4 \pm 2.2 \times 10^{-6}$, the values
for material at secular equilibrium with the bulk earth $^{232}\text{Th}/^{238}\text{U}$ value of 3.8. The corrections
are small because the uranium concentrations are high (~6 ppm) and detrital ^{232}Th components
190 are low (average <170 ppt) in both the samples (Supplementary Table 1).

2.5 Age models

We obtained 18 and 5 ^{230}Th dates for samples ML. 1 and ML. 2, respectively. The
average dating resolution for ML.1 is ~40 years with a precision of $\sim \pm 13$ years. In addition,
195 the portion of the 4.2 ka BP event (between 27 and 88 mm depth in ML.1) is constrained by a
total of 9 ^{230}Th dates with the average spacing of 7 mm between successive dates. All the dates
are in chronological order within an average dating uncertainty of ± 12 years. The ML.1 and
ML.2 age models and associated uncertainties were constructed using COPRA (Constructing
Proxy Records from Age model) (Breitenbach et al., 2012), Bchron (Haslett et al., 2008) and
200 ISCAM (Fohlmeister, 2012) age modeling schemes (Fig. 3), respectively. All three modeling
schemes yielded nearly identical age models and the conclusions of this study are not sensitive
to the choice of the age models (Fig. 3).



205 2.6 Stable isotope analysis

The ML.1 and ML.2 $\delta^{18}\text{O}$ records are established by ~970 and ~238 stable isotope measurements, respectively (Fig. 4, Supplementary Table 2).

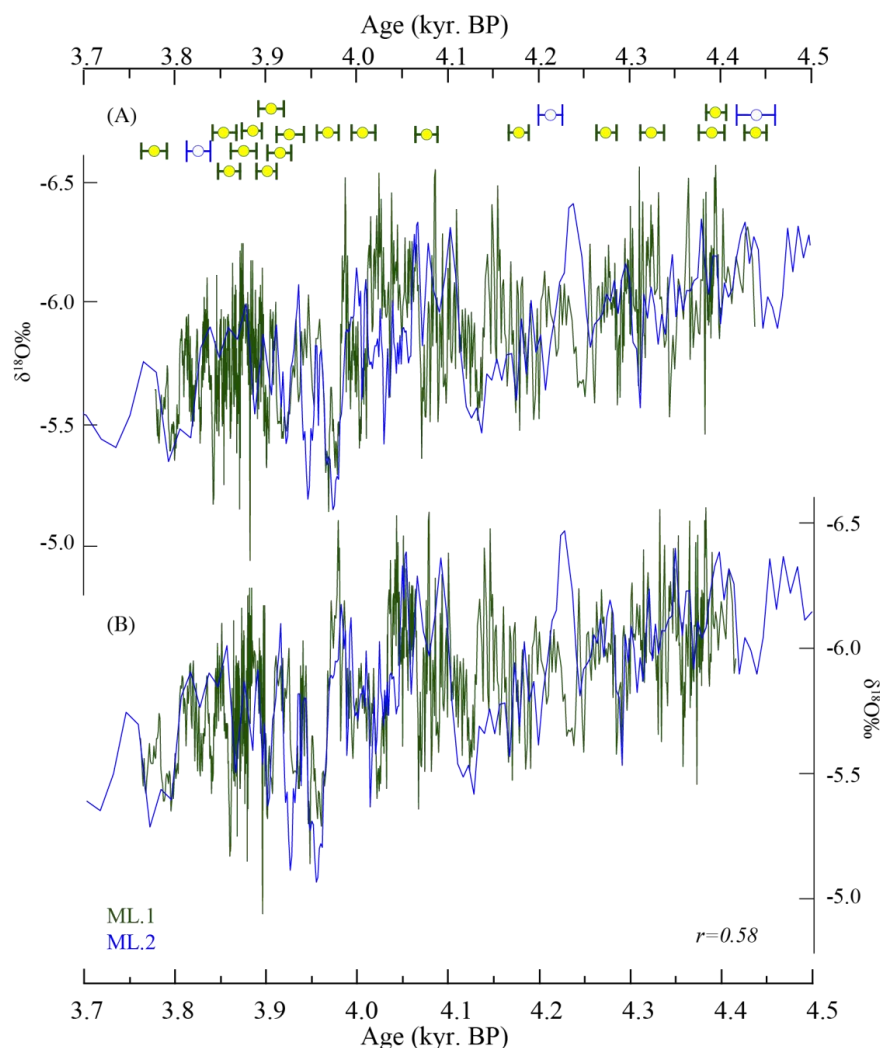


Figure 4. Comparison between ML.1 and ML.2 $\delta^{18}\text{O}$ records over the period of overlap.
210 The ML.1 and ML.2 $\delta^{18}\text{O}$ profiles replicate convincingly over the period of overlap, but with
some offset between their absolute $\delta^{18}\text{O}$ values (see text). The horizontal error bars on ^{230}Th
dates represent a 2σ analytical error. (A) The raw data of ML.1 (green) and ML.2 (blue)
samples on independent COPRA age model, the horizontal error bars depict ^{230}Th dates and
errors (2σ). (B) We used intra-site correlation age modeling (ISCAM) algorithm (Fohlmeister,
215 2012) to find the best correlation between ML.1 and ML.2 profiles (also see, Supplementary
Table 2).



We used New Wave Micromill, a digitally controlled tri-axial micromill equipment, to obtain subsamples. The subsamples (~80 μg) were continuously micromilled from ML. 1 and ML. 2 with typical increments between 50 and 100 μm (dependent on growth-rates) along the stalagmites growth axes. The $\delta^{18}\text{O}$ and $\delta^{13}\text{C}$ were measured using Finnigan MAT-253 mass spectrometer coupled with an on-line carbonate preparation system (Kiel-IV) in the Isotope Laboratory, Xi'an Jiaotong University. Results are reported in per mil (‰) relative to the Vienna PeeDee Belemnite (VPDB) standard. Duplicate measurements of standards NBS19 and TTB1 show a long-term reproducibility of ~0.1‰ (1 σ) or better.

225

2.7 Replication

We assessed the replication between ML.1 and ML.2 $\delta^{18}\text{O}$ records by using the ISCAM (Intra-Site Correlation Age Modeling) algorithm (Fohlmeister, 2012). The ISCAM finds the best correlation between the proxy records by using a Monte Carlo approach. Significant levels were calculated against a red-noise background from 1,000 pairs of artificially simulated first-order autoregressive time series (AR1). The ML.1 and ML.2 $\delta^{18}\text{O}$ time series on ISCAM derived age models display a statistically significant correlation ($r = 0.58$ at 95% confidence level) during their contemporary growth period between ~4.4–3.8 ka BP. The minor discrepancies between the two profiles may result from slight differences in their ^{230}Th dating resolution and/or growth rate variations (Fig. 4).

235

3 Results and Discussion

3.1 Results

The ML.1 and ML.2 $\delta^{18}\text{O}$ values range between -6.6‰ and -4.4‰ with mean values of -5.80‰ and -5.43‰, respectively. A slight but systematic offset in the mean $\delta^{18}\text{O}$ values of 0.4‰ between the two records may possibly stem from karst-related difference in the drip and /or degassing rates. Temporal resolutions of the ML.1 record range from ~0.1 to ~3 years with an average resolution of ~1 year. The average temporal resolution of the ML.2 record is ~5 years (Figs. 4 and 5).

245



3.2 Comparisons between KM-A and ML.1 and ML.2 $\delta^{18}\text{O}$ records

The ML.1 and ML.2 $\delta^{18}\text{O}$ record displays broad similarities with the previous KM-A $\delta^{18}\text{O}$ record from the same cave (Berkelhammer et al., 2012) but some differences are also evident (Fig. 5).

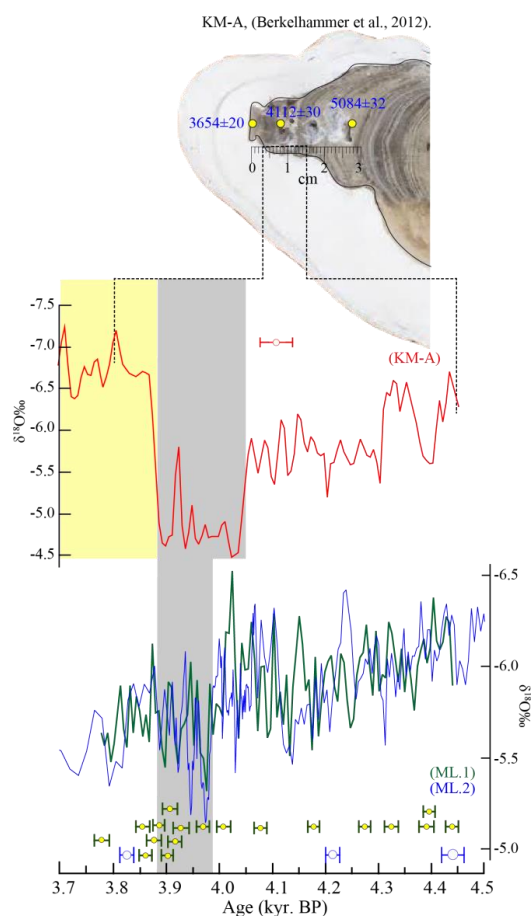


Figure 5. Comparison between KM-A and ML.1, ML.2: The KM-A stalagmite sample picture from Mawmluh cave (Berkelhammer et al., 2012). The 4.2 ka event occurs at the top portion of the sample (0-29 mm) which tapers towards the top and is constrained by three ^{230}Th dates (yellow dots). The dotted lines indicate the $\delta^{18}\text{O}$ depth from 4400 to 3654 years BP on the KM-A sample. Previously published stalagmite (KM-A) $\delta^{18}\text{O}$ record (red) from Mawmluh Cave (Berkelhammer et al., 2012). The raw $\delta^{18}\text{O}$ profile (blue) from ML.2 (this study) is overlaid by 6-years interpolated $\delta^{18}\text{O}$ profile (green) of ML.1 (this study, also see, Supplementary Table 2). The horizontal error bars (red, green and blue) on the ^{230}Th dates represent a 2σ analytical error. The vertical grey bar indicates the duration of the weak (driest phase) ISM variability recorded between KM-A and ML $\delta^{18}\text{O}$ profiles. The yellow bar indicates the anomalously depleted $\delta^{18}\text{O}$ values in KM-A record.



265 The ‘4.2 ka event’ in the KM-A record manifest as a two-step change, marked by an initial
increase in $\delta^{18}\text{O}$ values ($\sim 0.6\%$) between ~ 4.315 and 4.303 ka followed by a second and more
abrupt increase between ~ 4.071 and 4.049 ka BP. The latter is characterized by the most
enriched $\delta^{18}\text{O}$ values over the entire record ($\sim 1.5\%$ higher than the background values before
the event) (Fig. 5). The timing of most significant increase in both ML.1 and ML.2 $\delta^{18}\text{O}$ values
270 is similar to that observed in the KM-A profile (within the margin of age uncertainties) however,
the amplitudes of $\delta^{18}\text{O}$ change in our records are smaller by $\sim 0.5\%$ relative to the KM-A
profile (Fig. 5). The key difference between our and the KM-A records however, is the absence
of a sharp decrease in the $\delta^{18}\text{O}$ values in ML.1/ML.2 profiles after 3.88 ka BP, which mark the
termination of 4.2 ka event in the KM-A record. In contrast, the ML.1/ML.2 profiles exhibit a
275 longer-term gradual increase in the $\delta^{18}\text{O}$ values throughout the entirety of the record,
punctuated by several intervals of anomalously enriched $\delta^{18}\text{O}$ values. One plausible
explanation of the apparent differences between the two records could stem from partial
dissolution of top most portion of KM-A sample (Fig. 5), where the most depleted $\delta^{18}\text{O}$ values
were recorded. This is evident from deposition of a layer of white aragonite that apparently
280 occurred in the recent several decades after at the top of the old portion of the KM-A stalagmite
(Fig. 5), implying a possibility that the structure of the ‘4.2 ka event’ in the KM-A record could
have been altered to some extent. It is unlikely this affected the onset of the event, as it is
consistent between all record, but it does suggest the event may be better described as a “regime
shift” as opposed to a “pulse”.

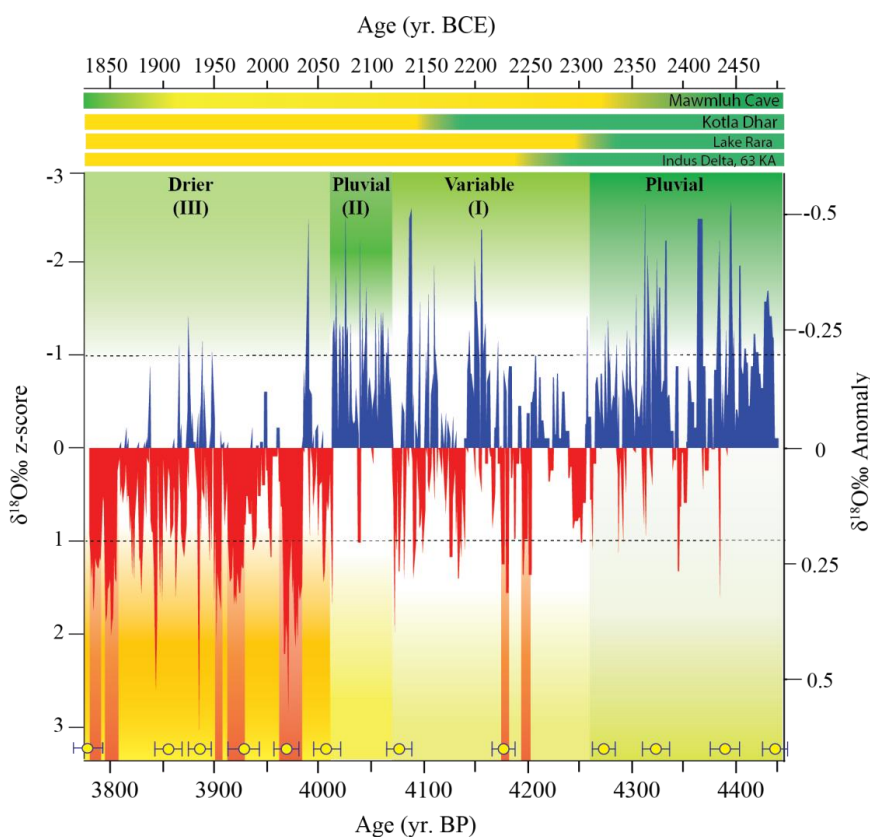
285

3.3 The ISM variability between 4.440 and 3.778 ka BP

A three-phase sequence of changes in the ML.1 $\delta^{18}\text{O}$ record (Fig. 6) characterize the structure
of the ‘4.2 ka event’ in the ISM domain (Fig. 6). The first phase is marked by an abrupt
transition at ~ 4.255 ka BP from a pluvial-like condition (i.e., lower $\delta^{18}\text{O}$) to highly variable
290 ISM (dry/wet) state that lasted for ~ 185 years (Fig. 6). This pattern of change in ISM is broadly
consistent with other proxy records from the ISM region (e.g., Staubwasser et al., 2003;
Kathayat et al., 2017). Within this phase, we infer the presence of two distinct decadal-length
droughts (see Fig. 6 for definition) centered at about ~ 4.2 ka BP (~ 13 years) and ~ 4.175 ka BP
(~ 10 years), respectively (Fig. 6). The second phase, between ~ 4070 and ~ 4010 years BP, is
295 marked by persistently depleted $\delta^{18}\text{O}$ values indicating a relatively stronger ISM period of ~ 60
years (Fig. 6). The third phase of the 4.2 ka event in ML.1 record is marked by an abrupt



weakening of ISM at ~ 4.01 ka BP inferred by $\sim 1.0\text{‰}$ shift in the $\delta^{18}\text{O}$ from -6.5‰ to -5.5‰ (Fig. 4) within ~ 10 years. Notably, this phase is punctuated by two multidecadal weak monsoon events centered at ~ 3.970 (~ 20 years) and ~ 3.915 (~ 25 years) ka BP, respectively (Fig. 6). Overall, the ML.1 record suggest that ISM was generally weaker between 3.8 and 4.0 ka BP and intermittently experienced multidecadal droughts rather than a sustained multicentennial episode of drought as commonly inferred from previous ISM reconstructions.



305 **Figure 6. The inferred ISM variability during the 4.2 ka BP Event:** The ML.1 $\delta^{18}\text{O}$ record is shown as z-score and anomaly (with respect to the mean $\delta^{18}\text{O}$ value of the entire record). The vertical shaded bars denote inferred periods of drier, pluvial and variable conditions. The horizontal shaded bar indicated the transition timing from pluvial to drier in other proxy records mentioned in the text (also see Figure 1). The dotted black dash lines indicate the 1 standard deviations. The vertical red bars delineate the inferred periods of the droughts (z-score > 1).
 310 The horizontal error bars show a subset of ^{230}Th dates with 2σ analytical error (for complete listing of ^{230}Th dates, see Supplementary Table 1).



315 **4 Conclusions**

The ML.1/ML.2 records from Mawmluh Cave, Northeast India provide a new record of ISM covering the period from ~4.440 to 3.780 ka BP. The record has unprecedented high-resolution (annual) and precise age control ($\sim\pm 13$ years), thus characterizes the timing and structure of the '4.2 ka event' in much more detail. It is now evident that the '4.2 ka event' in
320 Northeast India displays a three-phase structure: a dry (weak ISM) – wet (strong ISM) – dry (weak ISM) rhythm corresponding to the first (~4.255–4.070 ka BP), second (~4.070–4.012 ka BP) and third (~4.020–3.890 ka BP) phases, respectively as inferred from the $\delta^{18}\text{O}$ records. The new record also provides the most precise ISM variability up till now in the time range, which may potentially play a critical role in correlating and calibrating the climate variability
325 around the '4.2 ka event' globally.

330 **5 Author Contributions**

G.K. and H.C. designed the research and experiments. GK wrote the first draft of the manuscript. H.C. A.S. and M.B. revised the manuscript. G.K., H.C. and L.X.L. did the fieldwork and collected the samples. G.K., H.C., H.W.Z., and R.L.E. conducted the ^{230}Th dating. G.K., P.Z.D. and L.H.Y conducted the oxygen isotope measurements. All authors
335 discussed the results and provided inputs on the manuscript.

6 Competing interests

The authors declare no competing financial interests.
340

7 Acknowledgments

We thank D.S. Chauhan, C.S. Chauhan, A.S. Kathayat, G. Kathayat, N. Pant, S. Melkani, C. Dunnai, A. Dunnai, and C.J. Dunnai for their assistance during the fieldwork. **Funding:** This
345 work is supported by grants from Natural Science Foundation of China to G.K. (NSFC 41731174), H.C. (NSFC 41731174 and 4157020432) and H.W.Z. (NSFC 41502166).

8 Data and materials availability

All data needed to evaluate the conclusions in the paper are presented in the paper. Additional data related to this paper may be requested from the authors. The data will be archived at the NOAA National Climate Data Center (<https://www.ncdc.noaa.gov/data-access/paleoclimatology-data>). Correspondence and requests for materials should be addressed to G.K. (kathayat@xjtu.edu.cn) and H.C. (cheng021@xjtu.edu.cn).
355



References:

- Arz, H.W., Lamy, F., Pätzold, J.: A pronounced dry event recorded around 4.2 ka in brine sediments from the northern Red Sea. *Quaternary Research* 66, 432–441, 2006.
- Berkelhammer, M., Sinha, A., Stott, L., Cheng, H., Pausata, F., Yoshimura, K.: An abrupt shift in the Indian monsoon 4000 years ago. *Climates, landscapes, and civilizations*, 75–88, 2012.
- 360 Breitenbach, S.F., Adkins, J.F., Meyer, H., Marwan, N., Kumar, K.K., Haug, G.H.: Strong influence of water vapor source dynamics on stable isotopes in precipitation observed in Southern Meghalaya, NE India. *Earth and Planetary Science Letters* 292, 212–220, 2010.
- Breitenbach, S.F.M., Rehfeld, K., Goswami, B., Baldini, J.U.L., Ridley, H.E., Kennett, D.J., Pruffer, K.M., Aquino, V.V., Asmerom, Y., Polyak, V.J., Cheng, H., Kurths, J., Marwan, N.: COConstructing Proxy Records from Age models (COPRA). *Clim. Past* 8, 1765–1779, 2012.
- 365 Breitenbach, S.F.M., Lechleitner, F.A., Meyer, H., Diengdoh, G., Matthey, D., Marwan, N.: Cave ventilation and rainfall signals in dripwater in a monsoonal setting – a monitoring study from NE India. *Chemical Geology* 402, 111–124, 2015.
- 370 Chang K.C.: China on the eve of the Historical Period. In: Loewe M and and Shaughnessy EL (eds) *The Cambridge History of Ancient China – From the Origins of Civilization to 221 BC*. New York: Cambridge University Press, pp. 37–73, (1999).
- Cheng, H., Edwards, R., Hoff, J., Gallup, C., Richards, D., Asmerom, Y.: The half-lives of uranium-234 and thorium-230. *Chemical Geology* 169, 17–33, 2000.
- 375 Cheng, H., Zhang, P., Spötl, C., Edwards, R., Cai, Y., Zhang, D., Sang, W., Tan, M., An, Z.: The climatic cyclicity in semiarid-arid central Asia over the past 500,000 years. *Geophysical Research Letters* 39, 2012.
- Cheng, H., Edwards, R.L., Shen, C.-C., Polyak, V.J., Asmerom, Y., Woodhead, J., Hellstrom, J., Wang, Y., Kong, X., Spötl, C.: Improvements in ²³⁰Th dating, ²³⁰Th and ²³⁴U half-life values, and U–Th isotopic measurements by multi-collector inductively coupled plasma mass spectrometry. *Earth and Planetary Science Letters* 371, 82–91, 2013.
- 380 Cheng, H., Sinha, A., Verheyden, S., Nader, F.H., Li, X.L., Zhang, P.Z., Yin, J.J., Yi, L., Peng, Y.B., Rao, Z.G., Ning, Y.F., Edwards, R.L.: The climate variability in northern Levant over the past 20,000 years. *Geophysical Research Letters* 42, 8641–8650, 2015.
- 385 Cheng, H., Edwards, R.L., Sinha, A., Spötl, C., Yi, L., Chen, S., Kelly, M., Kathayat, G., Wang, X., Li, X.: The Asian monsoon over the past 640,000 years and ice age terminations. *Nature* 534, 640–646, 2016.
- Cullen, H.M., Hemming, S., Hemming, G., Brown, F., Guilderson, T., Sirocko, F.: Climate change and the collapse of the Akkadian empire: Evidence from the deep sea. *Geology* 28, 379–382, 2000.



- 390 Dayem, K. E., Molnar, P., Battisti, D. S., & Roe, G. H.: Lessons learned from oxygen isotopes in modern precipitation applied to interpretation of speleothem records of paleoclimate from eastern Asia. *Earth and Planetary Science Letters*, 295(1), 219–230, 2010.
- Dixit, Y., Hodell, D.A., Giesche, A., Tandon, S.K., Gázquez, F., Saini, H.S., Skinner, L.C., Mujtaba, S.A., Pawar, V., Singh, R.N.: Intensified summer monsoon and the urbanization of Indus
395 Civilization in northwest India. *Scientific reports* 8, 4225–, 2018.
- Dixit, Y., Hodell, D.A., Petrie, C.A.: Abrupt weakening of the summer monsoon in northwest India~4100 yr ago. *Geology* 42, 339–342, 2014.
- Drysdale, R., Zanchetta, G., Hellstrom, J., Maas, R., Fallick, A., Pickett, M., Cartwright, I., Piccini, L.:
400 Late Holocene drought responsible for the collapse of Old World civilizations is recorded in an Italian cave flowstone. *Geology* 34, 101–104, 2006.
- Dutt, S., Gupta, A. K., Clemens, S. C., Cheng, H., Singh, R. K., Kathayat, G., & Edwards, R. L.: Abrupt changes in Indian summer monsoon strength during 33,800 to 5500 years BP. *Geophysical Research Letters*, 42(13), 5526–5532, 2015
- Edwards, R.L., Chen, J., Wasserburg, G.: ²³⁸U ²³⁴U ²³⁰Th ²³²Th systematics and the precise
405 measurement of time over the past 500,000 years. *Earth and Planetary Science Letters* 81, 175–192, 1987.
- Enzel, Y., Ely, L.L., Mishra, S., Ramesh, R., Amit, R., Lazar, B., Rajaguru, S.N., Baker, V.R., Sandler, A.: High-resolution Holocene environmental changes in the Thar Desert, northwestern India. *Science* 284, 125–128, 1999.
- 410 Fohlmeister, J.: A statistical approach to construct composite climate records of dated archives. *Quaternary Geochronology* 14, 48–56, 2012.
- Giosan, L., Clift, P.D., Macklin, M.G., Fuller, D.Q., Constantinescu, S., Durcan, J.A., Stevens, T., Duller, G.A., Tabrez, A.R., Gangal, K.: Fluvial landscapes of the Harappan civilization. *Proceedings of the National Academy of Sciences* 109, E1688–E1694, 2012.
- 415 Haslett, J., Parnell, A.: A simple monotone process with application to radiocarbon-dated depth chronologies. *Journal of the Royal Statistical Society: Series C (Applied Statistics)* 57, 399–418, 2008.
- Hong, B., Hong, Y., Uchida, M., Shibata, Y., Cai, C., Peng, H., Zhu, Y., Wang, Y., Yuan, L.: Abrupt variations of Indian and East Asian summer monsoons during the last deglacial stadial and
420 interstadial. *Quaternary Science Reviews* 97, 58–70, 2014.
- Hong, B., Uchida, M., Hong, Y., Peng, H., Kondo, M., Ding, H.: The respective characteristics of millennial-scale changes of the India summer monsoon in the Holocene and the Last Glacial. *Palaeogeography, Palaeoclimatology, Palaeoecology* 496, 155–165, 2018.
- Kathayat, G., Cheng, H., Sinha, A., Spötl, C., Edwards, R.L., Zhang, H., Li, X., Yi, L., Ning, Y., Cai,
425 Y., Lui, W.L., Breitenbach, S.F.M.: Indian monsoon variability on millennial-orbital timescales. *Scientific Reports* 6, 24374, 2016.



- Kathayat, G., Cheng, H., Sinha, A., Yi, L., Li, X., Zhang, H., Li, H., Ning, Y., Edwards, R.L.: The Indian monsoon variability and civilization changes in the Indian subcontinent. *Science advances* 3, e1701296, 2017.
- 430 Liu, F., Feng, Z.: A dramatic climatic transition at ~4000 cal. yr BP and its cultural responses in Chinese cultural domains. *Holocene* 22, 1181e1197, 2012.
- Madella, M., Fuller, D.Q.: Palaeoecology and the Harappan Civilisation of South Asia: a reconsideration. *Quaternary Science Reviews* 25, 1283–1301, 2006.
- Marshall, M.H., Lamb, H.F., Huws, D., Davies, S.J., Bates, R., Bloemendal, J., Boyle, J., Leng, M.J.,
435 Umer, M., Bryant, C.: Late Pleistocene and Holocene drought events at Lake Tana, the source of the Blue Nile. *Global and Planetary Change* 78, 147–161, 2011.
- Menounos, B., Clague, J.J., Osborn, G., Luckman, B.H., Lakeman, T.R., Minkus, R.: Western Canadian glaciers advance in concert with climate change circa 4.2 ka. *Geophysical Research Letters* 35, 2008.
- 440 Midhun, M., & Ramesh, R.: Validation of $\delta^{18}\text{O}$ as a proxy for past monsoon rain by multi-GCM simulations. *Climate dynamics*, 46(5-6), 1371–1385, 2016.
- Murata, F., Hayashi, T., Matsumoto, J., Asada, H.: Rainfall on the Meghalaya plateau in northeastern India—one of the rainiest places in the world. *Natural Hazards* 42, 391–399, 2007.
- Myers, C.G., Oster, J.L., Sharp, W.D., Bennartz, R., Kelley, N.P., Covey, A.K., Breitenbach, S.F.:
445 Northeast Indian stalagmite records Pacific decadal climate change: Implications for moisture transport and drought in India. *Geophysical Research Letters* 42, 4124–4132, 2015.
- Nakamura, A., Yokoyama, Y., Maemoku, H., Yagi, H., Okamura, M., Matsuoka, H., Miyake, N., Osada, T., Adhikari, D.P., Dangol, V.: Weak monsoon event at 4.2 ka recorded in sediment from Lake Rara, Himalayas. *Quaternary International* 397, 349–359, 2016.
- 450 Pausata, F. S., Battisti, D. S., Nisancioglu, K. H., & Bitz, C. M.: Chinese stalagmite $[\delta^{18}\text{O}]$ 180 controlled by changes in the Indian monsoon during a simulated Heinrich event. *Nature Geoscience*, 4(7), 474–480., 2011.
- Ponton, C., Giosan, L., Eglinton, T.I., Fuller, D.Q., Johnson, J.E., Kumar, P., Collett, T.S.: Holocene aridification of India. *Geophysical Research Letters* 39, 2012.
- 455 Prasad, S., Enzel, Y.: Holocene paleoclimates of India. *Quaternary Research* 66, 442–453, 2006.
- Railsback, L.B., Liang, F., Brook, G., Voarintsoa, N.R.G., Sletten, H.R., Marais, E., Hardt, B., Cheng, H., Edwards, R.L.: The timing, two-pulsed nature, and variable climatic expression of the 4.2 ka event: A review and new high-resolution stalagmite data from Namibia. *Quaternary Science Reviews* 186, 78–90, 2018.
- 460 Sabin, T., Krishnan, R., Ghattas, J., Denvil, S., Dufresne, J.-L., Hourdin, F., Pascal, T.: High resolution simulation of the South Asian monsoon using a variable resolution global climate model. *Climate dynamics* 41, 173–194, 2013.



- 465 Sengupta, S., Sarkar, A.: Stable isotope evidence of dual (Arabian Sea and Bay of Bengal) vapour sources in monsoonal precipitation over north India. *Earth and Planetary Science Letters* 250, 511–521, 2006.
- Shukla, T., Mehta, M., Jaiswal, M.K., Srivastava, P., Dobhal, D., Nainwal, H., Singh, A.K.: Late Quaternary glaciation history of monsoon-dominated Dingad basin, central Himalaya, India. *Quaternary Science Reviews* 181, 43-64, 2018.
- 470 Sinha, A., Kathayat, G., Cheng, H., Breitenbach, S.F., Berkelhammer, M., Mudelsee, M., Biswas, J., Edwards, R.: Trends and oscillations in the Indian summer monsoon rainfall over the last two millennia. *Nature communications* 6, 2015.
- Sinha, A., Berkelhammer, M., Stott, L., Mudelsee, M., Cheng, H., Biswas, J.: The leading mode of Indian Summer Monsoon precipitation variability during the last millennium. *Geophysical Research Letters* 38, 2011
- 475 Stanley, J.-D., Krom, M.D., Cliff, R.A., Woodward, J.C.: Nile flow failure at the end of the Old Kingdom, Egypt: strontium isotopic and petrologic evidence. *Geoarchaeology: Int. J.* 18, 395e402, 2003.
- Staubwasser, M., Sirocko, F., Grootes, P., Segl, M.: Climate change at the 4.2 ka BP termination of the Indus valley civilization and Holocene south Asian monsoon variability. *Geophysical Research Letters* 30, 2003.
- 480 Vuille, M., Werner, M., Bradley, R. S., & Keimig, F.: Stable isotopes in precipitation in the Asian monsoon region. *Journal of Geophysical Research: Atmospheres*, 110(D23), n/a-n/a. doi: 10.1029/2005JD006022, 2005.
- Weiss, H.: Global megadrought, societal collapse and resilience at 4.2-3.9 ka BP across the mediterranean and west asia. *PAGES* 24, 62–63, 2016.
- 485 Weiss, H., Courty, M.-A., Wetterstrom, W., Guichard, F., Senior, L., Meadow, R., Curnow, A.: The genesis and collapse of third millennium north Mesopotamian civilization. *Science* 261, 995–1004, 1993.